ETAC/CBT
FILE COPY
13 SEP 1976

~~EDDA~~
~~76-3~~
02410,
02421

NOAA Technical Mem EDS-CEDDA-TM-9

AN EVALUATION OF THE METEOROLOGICAL DATA FROM THE GATE BOUNDARY LAYER INSTRUMENT SYSTEM (BLIS)

Center for Experiment
Design and Data Analysis
Washington, D. C.
July 1976

noaa NATIONAL OCEANIC AND ATMOSPHERIC ADMINISTRATION / Environmental Data Service

NOAA TECHNICAL MEMORANDUMS
Environmental Data Service, CEDDA Series

The Center for Experiment Design and Data Analysis (CEDDA) became part of NOAA's Environmental Data Service in 1972 and was given the responsibility for data management and research activities related to major international scientific field experiments.

Formerly the Barbados Oceanographic and Meteorological Analysis Project (BOMAP), CEDDA is still concerned with analyses of data collected during the Barbados Oceanographic and Meteorological Experiment (BOMEX), conducted in 1969, and will continue to issue publications pertaining to BOMEX as part of the EDS BOMAP series.

NOAA Technical Memorandums in the Environmental Data Service CEDDA series will serve to disseminate information related to the 1972-73 International Field Year for the Great Lakes (IFYGL), the 1974 Global Atmospheric Research Program (GARP) Atlantic Tropical Experiment (GATE), as well as other projects in which CEDDA participates.

Publications listed below are available from the National Technical Information Service, U.S. Department of Commerce, Sills Bldg., 5285 Port Royal Road, Springfield, Va. 22151. Prices on request. Order by accession number (given in parentheses).

NOAA Technical Memorandums

EDS CEDDA-1	Omega Wind-Finding Capabilities: Wallops Island Experiments. Donald T. Acheson, October 1973, 77 pp. (COM-74-10039)
EDS CEDDA-2	Characteristics of the Lower Atmosphere Near Saipan, April 29 to May 16, 1945. Joshua Z. Holland, April 1975, 24 pp. (PB246-962)
EDS CEDDA-3	IFYGL Physical Data Collection System: Intercomparison Data. Jack Foreman, May 1975, 7 pp. (COM-75-10907)
EDS CEDDA-4	Preliminary Report on Wind Errors Encountered During Automatic Processing of IFYGL LORAN-C Data. J. Sullivan and J. Matejceck, May 1975, 9 pp. (COM-75-10908)
EDS CEDDA-5	Generation of GATE Ship Speed Data by Variational Technique. Jerry Sullivan, June 1975, 5 pp. (COM-75-10995)
EDS CEDDA-6	Data Editing--Subroutine EDITQ. Donald T. Acheson, June 1975, 12 pp.
EDS CEDDA-7	Thermal Time Constants of U.S. Radiosonde Sensors Used in GATE. Scott L. Williams and Donald T. Acheson, May 1976, 16 pp.

(Continued on inside back cover)

QC
807.5
.U6
C4
no.9

#4506621

NOAA Technical Memorandum EDS CEDDA-9

AN EVALUATION OF THE METEOROLOGICAL DATA FROM THE GATE BOUNDARY LAYER INSTRUMENT SYSTEM (BLIS)

C. F. Ropelewski

Center for Experiment
Design and Data Analysis
Washington, D.C.
July 1976

30 SEP 1997

UNITED STATES
DEPARTMENT OF COMMERCE
Elliot L. Richardson, Secretary

NATIONAL OCEANIC AND
ATMOSPHERIC ADMINISTRATION
Robert M. White, Administrator

Environmental Data
Service
Thomas S. Austin, Director

AWS TECHNICAL LIBRARY
FL 4414
859 BUCHANAN STREET
SCOTT AFB IL 62225-5118

CONTENTS

Page

Abstract 1

1. Introduction 1

2. Instrumentation and Data 2

3. Error Analysis 3

   A. Interchannel Biases 5

   B. Intersonde Biases 7

   C. Typical Rms Errors 7

4. Coherence and Spectral Analysis 10

   A. Wind Speed 10

   B. Wind Direction 12

   C. Tilt Angle 15

5. Profiles 15

   A. Dry-bulb Temperature 17

   B. Wet-bulb Temperature 18

   C. Wind Speed 8

6. Discussion 19

Acknowledgment 21

References 21

Appendix 23

List of Figures

Page

Figure 1.--The GATE Boundary Layer Instrument System 2

Figure 2.--Comparison of measured relative humidity, RH1, and calculated relative humidity, RH2 10

Figure 3.--Wind speed spectra and coherence; 0.25-sps data; interchannel; height, 100 m. 11

Figure 4.--Wind speed spectra and coherence; 0.25-sps data; interchannel; height, 400 m. 12

Figure 5.--Wind speed spectra and coherence; 0.5-sps data; intersonde; height, 100 m. 13

Figure 6.--Wind speed spectra and coherence; 0.5-sps data; intersonde; height, 400 m. 13

Figure 7.--Wind direction spectra and coherence; 0.5-sps data; intersonde; height, 100 m. 14

Figure 8.--Wind direction spectra and coherence; 0.5-sps data; intersonde; height, 400 m. 15

Figure 9.--Tilt angle spectra and coherence; 0.25-sps data; interchannel; height, 100 m. 16

Figure 10.--Tilt angle spectra and coherence; 0.5-sps data; intersonde; height, 100 m. 16

Figure 11.--Tilt angle spectra and coherence; 0.5-sps data; intersonde; height, 400 m. 17

Figure 12.--Dry-bulb temperature profiles; *Researcher* flight 51; ascent. 18

Figure 13.--Dry-bulb temperature profiles; *Researcher* flight 51; descent 19

Figure 14.--Wet-bulb temperature profiles; *Researcher* flight 51; ascent. 20

Figure 15.--Wet-bulb temperature profiles; *Researcher* flight 51; descent 21

Figure 16.--Wind speed profiles; *Researcher* flight 51; ascent 22

Figure 17.--Wind speed profiles; *Researcher* flight 51; descent . . . 23

AN EVALUATION OF THE METEOROLOGICAL DATA FROM THE GATE BOUNDARY LAYER INSTRUMENT SYSTEM (BLIS)

C. F. Ropelewski
Center for Experiment Design and Data Analysis,
Environmental Data Service
National Oceanic and Atmospheric Administration
Washington, D.C. 20235

ABSTRACT. Comparisons are made of data obtained with the Boundary Layer Instrument System (BLIS), a tethered sonde, during the GARP Atlantic Tropical Experiment (GATE) in 1974. Based on data from 20 sondes, spectra of wind variables and effects of balloon and ship motion of the wind data are discussed, several profiles are compared, and estimates of typical sensor biases and rms errors are presented.

1. INTRODUCTION

Instrumented towers and aircraft have been used extensively to probe the planetary boundary layer. Direct measurements in the boundary layer may also be obtained with a less widely used instrument system, the tethered sonde. The relative advantages of each system are discussed in a paper by Readings (1975). A comparison of tower-mounted and tethered balloon instrumentation (Haugen et al. 1975) shows that most parameters of interest can be measured adequately with a tethered sonde. The present study is concerned with the evaluation of the data from a particular type of tethered sonde, the Boundary Layer Instrument System, (BLIS). The BLIS was used extensively during the GARP Atlantic Tropical Experiment (GATE) in 1974. This entirely new system was designed by the University of Wisconsin jointly with the National Oceanic and Atmospheric Administration (NOAA).

The BLIS was used during GATE by three United States ships: the Researcher, the Dallas, and the Oceanographer. Approximately 10,000 sonde hours of data were gathered during the experiment.

The discussion that follows is concerned with the internal consistency and quality of the BLIS data. No comparisons were made with other instruments, nor were any special corrections applied to the processed data selected. The purpose here is solely to present estimates of typical relative biases between sondes and of typical rms errors associated with the sensors, and to identify sources of error in the data. The analysis presented in this study serves not only as a guide for the use of the GATE BLIS data but also gives an indication of the capabilities and limitations of tethered sondes in boundary layer experiments.

2. INSTRUMENTATION AND DATA

The BLIS sonde is, in essence, a radiosonde that can be attached to the tether line of a balloon. A schematic of a BLIS sonde is shown in figure 1.

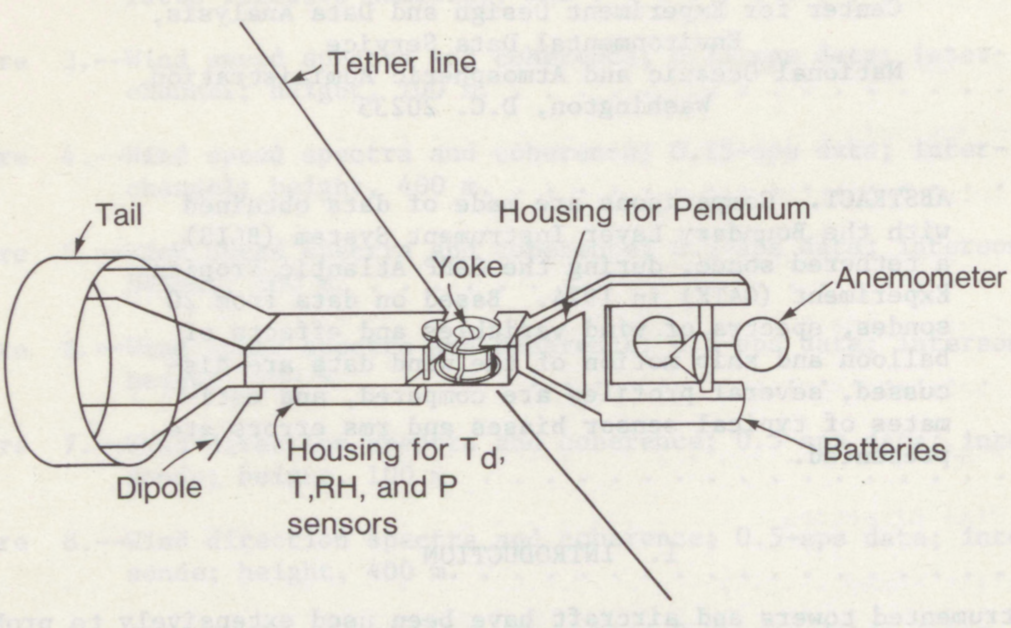

Figure 1.--The GATE Boundary Layer Instrument System

The sonde was attached to a ball of the tether line by a yoke, and was free to swivel in all directions in the horizontal and ±18° in the vertical. The parameters measured by the sonde and the sensors used to measure them are listed in table 1. A detailed description of the instrumentation, sensor design characteristics, and telemetry can be found in Burns (1974).

The temperatures, relative humidity, and pressure measurements were taken at a rate of one sample every 3.6 s and recorded every 4 s. Duplicate samples were eliminated in the data processing. The wind direction, speed, and tilt angle were sampled twice in 3.6 s. Each of the two samples were treated as entirely different variables and recorded on different data channels once every 4 s. These data, 3-min and hourly averages, and the documentation for the BLIS flights may be obtained from World Data Center A, National Climatic Center, Ashville, N.C.

Each of the three BLIS ships was equipped with a winch, for reeling out the tether line, the appropriate telemetry and recording systems, and a supply of balloons and sondes. The balloons were capable of lifting the sondes to a maximum altitude of 1400 m. As many as five sondes were flown at one time depending upon the mode of operation. There were two primary modes of operation; fixed level and profile. In the fixed level mode, several sondes were kept at a predetermined height for as long as 36 hr. In the profile mode, one or more sondes took continuous, or nearly continuous, soundings for periods up to 24 hr. The time required to sound up to 1400 m was in the order of 20 min. The mode of operation was determined by the synoptic situation

Table 1. BLIS sensors

Parameter	Sensor
Dry-bulb temperature	Bead thermistor
Wet-bulb temperature	Bead thermistor
Relative humidity	Carbon hygristor
Pressure	Aneroid barometer
Wind speed	Three-cup Aneomometer
Wind direction	Magnetodiode
Tilt Angle	Pendulum and photocells

and operational constraints. As far as was possible BLIS sondes were flown every day during the active GATE phases from each of the three ships.

The flights chosen for analysis were those in which two or more sondes were flown within 1 m of each other for periods of at least 1 hr. These flights are listed in table 2. All of the flights are fixed level mode flights except for Test Run 9. This run was included to give an example of data taken during the profile mode of operation. Data from 20 of the 54 sondes built for GATE are included in the study.

3. ERROR ANALYSIS

The instrument errors associated with each BLIS sensor are estimated in the following way. If X_i and Y_i are values of the same variable measured by two adjacent sensors, we can write

$$X_i = T_i + e_{xi} + B_x, \qquad (1)$$

and

$$Y_i = T_i + e_{yi} + B_y, \qquad (1b)$$

where T_i are the true values of the variable, e_{xi} and e_{yi} are the random errors associated with each sensor, and B_x and B_y are the biases in the two sensors.

The difference between the two measurements at any given time is

$$Z_i = X_i - Y_i = e_{xi} - e_{yi} + B, \qquad (2)$$

Table 2. BLIS flight information.

Test run No.	BLIS flight No.	Ship	GATE observation period	Date (1974)	Start time (GMT)	Duration (s)	Sonde No.
1	2	Researcher	Intercomparison I	Jun 17	1545	4096	10280 02184
2	64	Dallas	Intercomparison II	Aug 16	1416	4096	05268 06360
3	64	Dallas	Intercomparison II	Aug 16	1524	4096	05268 06360
4	73	Oceanographer	Intercomparison III	Sep 22	1308	4096	01220 07324
5	73	Oceanographer	Intercomparison III	Sep 22	1416	4096	01220 07324
6	52	Oceanographer	Phase III	Aug 31	1545	3600	12400 03140 07196
7	52	Oceanographer	Phase III	Aug 31	1645	3600	12400 03148 07196
8	53	Oceanographer	Phase III	Sep 1	0400	4800	01220 10480 12336
9	51	Researcher	Phase III	Sep 3	1930	3602 (Entire flight)	14520 04112 02184
10							09361 10280
10	59	Oceanographer	Phase III	Sep 5	1520	2048	13428 00192
11	59	Oceanographer	Phase III	Sep 5	1520	2048	14392 06232
12	68	Researcher	Phase III	Sep 14	1930	3600	04304 11372

where $B = B_x - B_y$ is the relative bias between the two sensors. The mean of Z_i is simply the relative bias between the two sensors, provided that the errors are truly random. If we now form a variable, d_i, by removing the relative bias between the sondes, the variance of the error associated with the instruments, S^2_e, can be estimated from the variance of the difference S^2_d. This can be seen by noting that

$$d_i = Z_i - B = e_{xi} - e_{yi}, \tag{3}$$

and the variance can then be written

$$S^2_d = \frac{1}{N} \Sigma (e_{xi} - e_{yi})^2 = 2S^2_e, \tag{4}$$

if $\overline{e_{xi} e_{yi}} = 0$ and $e_{xi}{}^2 = e_{yi}{}^2$, i.e., if the errors are uncorrelated and the sensors are identical. Thus the rms error associated with the sensors can be estimated as

$$S_e = \frac{1}{\sqrt{2}} S_d.$$

A. Interchannel Biases

Wind speed, wind direction, and tilt angle were recorded at 0.5 samples per second (sps), twice the sampling rate of the other parameters. The data acquisition system was designed to record data at 0.25-sps only; thus each of the wind variables were recorded on two different data channels to form two 0.25-sps time series. The 0.5-sps series can be reconstructed by taking data points from each channel, alternating between channels.

A comparison was made in order to see whether any biases were introduced by splitting the time series of the wind variables into two separate series. The resulting computed interchannel biases for 14 sondes are listed in table 3. As seen in this table, the largest interchannel bias in the wind speed was 0.02 m/s. The frequency distributions of the wind speeds from each channel were almost identical. Thus we can assume that there are no significant interchannel biases in the wind speed.

The wind directions show interchannel biases of up to 4°, which appear only on the flights made during the Intercomparison periods. The frequency distributions of the wind directions show that values far from the mean appear slightly more often in one channel for these flights. An examination of the time series shows that the interchannel biases are not due to transitions between angles near 0 and 360° but are a result of random jumps in the wind direction. There are no interchannel biases in the Phase III wind direction data, because these random direction jumps of up to 180° were edited or corrected in processing the BLIS data for Phase III.

The interchannel tilt angle bias is zero for 11 of the 14 sondes listed in table 3, and largest bias, 0.3°, is for a flight in which more than 40% of

Table 3. Interchannel sensor bias.

Run/Sonde No. No.	Speed $(m\ s^{-1})$ Channel 1	Speed $(m\ s^{-1})$ Channel 2	Speed $(m\ s^{-1})$ Difference (1-2)	Direction (deg) Channel 1	Direction (deg) Channel 2	Direction (deg) Difference (1-2)	Tilt angle (deg) Channel 1	Tilt angle (deg) Channel 2	Tilt angle (deg) Difference (1-2)
1/1	2.94	2.92	0.02	67	71	-4	6.9	7.1	-0.2
1/2	3.18	3.18	0.00	100	98	2	5.8	5.9	-0.1
2/1	5.16	5.16	0.00	273	273	0	-4.7	-4.7	0.0
2/2	5.23	5.23	0.00	257	257	0	8.1	8.1	0.0
3/1	5.89	5.89	0.00	301	301	0	-6.0	-6.0	0.0
3/2	5.99	5.99	0.00	252	252	0	6.3	6.3	0.0
4/1	3.11	3.11	0.00	174	174	0	1.3	1.3	0.0
4/2	3.15	3.15	0.00	192	190	2	-0.3	0.0	-0.3
5/1	1.36	1.36	0.00	188	187	1	-1.5	-1.5	0.0
5/2	1.38	1.38	0.00	194	198	-4	1.9	1.9	0.0
6/1	8.31	8.32	-0.01	222	222	0	0.0	0.0	-0.0
6/2	8.22	8.21	0.01	201	201	0	6.5	6.5	0.0
7/1	8.11	8.12	-0.01	213	213	0	6.5	6.5	0.0
7/2	8.18	8.17	0.01	214	214	0	3.7	3.7	0.0

the tilt angle data are missing and which therefore is not representative. The largest interchannel tilt angle bias to be expected, then, is 0.1 to 0.2°.

B. Intersonde Biases

When two or more sondes are flown very close to each other on the same tether line, the relative bias between the sensors can be estimated. The relative biases of measured variables for nine BLIS pairs are listed in table 4, where the wind estimates are based on the 0.5-sps data. The values listed in table 4 are typical of those found in many of the pre-and post-flight calibration checks.

Experience with processing the BLIS data for Phase III of GATE indicates that intersonde wind direction biases tend to remain constant once the random direction jumps referred to earlier, are removed.

The tilt angle biases may be ascribed to two different sources. First, the sondes may have varying equilibrium positions for different portions of the flight because of the varying amount of water in the wet-bulb tank. Second, the sondes have a tendency to remain in one attitude, "to stick," for portions of flights, or for entire flights. Since there is no way to predict the tilt angle biases caused by this or by the water-tank problem, the time series of the tilt angles should be examined carefully before any analysis of either the horizontal or the vertical wind component is attempted.

The relative pressure biases are not included in table 4. Most of them were removed as part of the data processing. It should be noted, however, that pressure sensor drifts of 5 mb and more have been observed. In addition, sudden jumps of up to 10 mb in the measured pressure have been identified in the time-series plots of the data. Thus the time series of the pressure should also be carefully examined before these data are used in analysis.

The relative humidity is measured directly with a carbon hygristor and may be calculated from the dry- and wet-bulb temperatures. An examination of several time series of the relative humidity from the BLIS hygristors shows that these instruments have a much faster response time than the dry- and wet-bulb thermisters. The hygristor relative humidity values tend to be slightly larger than the relative humidities derived from the dry- and wet-bulb data. An example is shown in figure 2. The relative difference between the measured and derived relative humidities appear to increase with higher relative humidity.

C. Typical Rms Errors

The rms errors associated with the sensors on several BLIS sondes were calculated by the method discussed above. These error estimates are listed in table 5 for 12 different sonde pairs on six flights. The error estimates for Run 9 which contains two profiles, are slightly larger than the estimates for the remaining, level, flights. This is to be expected, since the computation method is not entirely valid for this flight, which was taken in the profile mode.

Table 4. Typical biases between adjacent sensors.

Run No.	Intersonde difference (1-2) Temperature (°C) Dry bulb	Wet bulb	Relative humidity (%)	Wind Speed (m s^{-1})	Wind Direction (deg)	Tilt Angle (deg)
1	-0.48	-0.29	0.3	-0.24	-30	1.2
2	-0.25	0.29	0.5	-0.07	17	-12.8
3	-0.14	0.29	0.3	-0.10	48	-12.3
4	0.16	-0.08	-2.1	-0.04	-16	1.3
5	-0.07	-0.25	-2.1	-0.02	-9	-3.4
6	0.25	0.05	0.2	0.08	2	-4.2
7	0.18	0.03	0.5	0.06	0	-5.3
8	-0.19	0.12	1.5	-0.23	17	-4.8
9	0.02	0.14	-1.8	-0.09	0	5.5
10	0.04	-0.19	2.4	-0.05	-1	2.8
11	0.55	1.34	0.3	0.11	21	-6.4
12	-0.01	-0.03	-0.2	0.08	2	3.1

Table 5. Estimates of rms errors assoicated with each sensor.

Run No.	Sonde Pair	Temperature (^{o}C) Dry bulb	Temperature (^{o}C) Wet bulb	Relative humidity (%)	Wind speed ($m\ s^{-1}$)	Wind direction (deg)	Tilt angle (deg)	Pressure (mb)
6	1-2	M	0.1	0.8	0.20	3.4	5.0	0.2
6	1-3	0.1	0.1	0.4	0.17	4.3	1.6	0.2
7	1-2	M	0.1	1.0	0.17	M	0.3	0.3
7	1-3	0.1	0.1	0.5	0.22	3.8	2.2	0.4
8	1-2	(0.04)	0.1	0.1	0.22	10.2*	1.0	0.2
8	1-3	(0.04)	(0.04)	0.1	0.19	10.4*	1.2	0.2
9	1-2	0.1	0.1	1.5	0.22	4.7	3.7	1.4
9	3-2	0.1	0.1	0.6	0.18	4.2	2.1	0.7
9	4-2	0.1	0.1	0.4	0.38	3.5	5.3	0.8
9	5-2	0.1	0.1	0.4	0.29	4.8	3.0	0.2
11	1-2	0.1	0.1	0.3	0.16	3.6	0.8	0.1
12	1-2	0.1	0.1	0.3	0.36	2.7	1.5	0.7
	Mean	0.1	0.1	0.5	0.22	3.8	2.2	0.4

*Events Log entry indicates sonde direction sensor is "sticking"

M - Missing

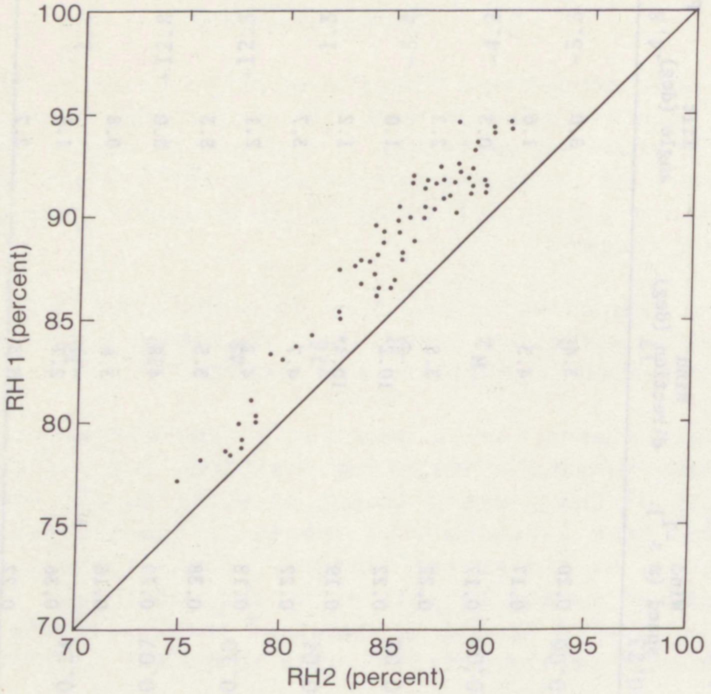

Figure 2.--Comparison of measured relative humidity, RH1, and calculated relative humidity, RH2.

The errors associated with the dry-bulb and wet-bulb temperatures, relative humidity, and wind speed are reasonably small, but the errors in the remaining variables could be significant for many types of analysis. For instance, the mean rms error in the tilt angle of 2.2° could amount to an uncertainty of as much as 0.4 m/s in the vertical velocity, w, for a wind speed of 10 m/s. Uncertainties of this magnitude in w severaly limit the use of the tilt angle data. Estimates of the rms errors in such derived variables as specific humidity and potential temperature are given in the Appendix.

4. COHERENCE AND SPECTRAL ANALYSIS

The wind speed, wind direction, and tilt angle data are particularly susceptible to contamination by ship and balloon motions. In this section the spectra of these variables are examined to ascertain the frequencies associated with such motions. The interchannel and intersonde coherence are also examined. Unless otherwise stated, the series were 4096 s long.

A. Wind Speed

The interchannel wind-speed coherence and spectra were calculated for each channel for several sondes. The sampling rate for these data was 0.25 sps. Sondes flown relatively near the surface had badly aliased wind speed spectra and poor interchannel coherence from midfrequencies (0.03 Hz) to the

AWS TECHNICAL LIBRARY
FL 4414
859 BUCHANAN STREET

Nyquist frequency. An example of the spectra and interchannel coherence for a sonde flown at 100 m is shown in figure 3. Sondes flown at greater heights showed an improvement in the interchannel coherence at midfrequencies. The aliasing in the spectra was also reduced for these flights (fig. 4, height of 400 m). The aliasing, particularly in the lower levels, is at least in part due to ship roll and pitch. These ship motions have periods of 6 to 12 s and thus are not well resolved by the 0.25-sps interchannel data.

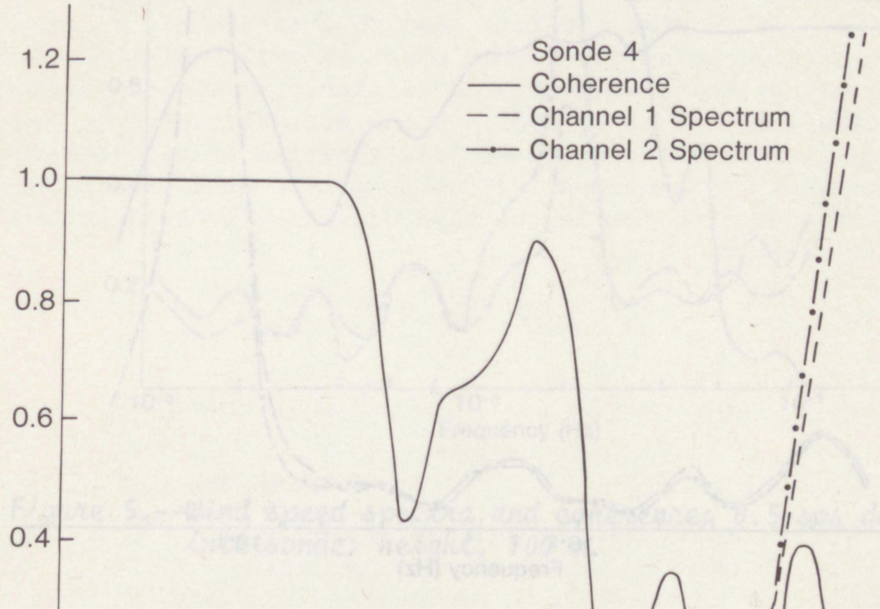

Figure 3.--Wind speed spectra and coherence; 0.25-sps data; interchannel; height, 100 m.

The separate channel time series of the wind were combined to form the 0.5-sps series for each sonde. The wind speed coherence between adjacent sondes and the spectra for each sonde were calculated. For sondes near the surface, the speed spectra for each sonde shows a high-frequency peak that can be attributed to ship motion. An example of this is seen in figure 5, which also shows the intersonde speed coherence for sondes near the surface. The coherence remains high throughout the entire frequency range. A similar spectral peak in the horizontal wind speed has also been attributed to ship motion by Berman (1976) in an analysis of BLIS data from the GATE International Sea Trials held in 1973.

For sondes at greater heights (400 m), the speed spectra in general, show no peak corresponding to the ship motion. These spectra, for example, figure 6, are slightly aliased but not as severely as the interchannel data at the same height. The intersonde coherence, shown in the same figure, re-

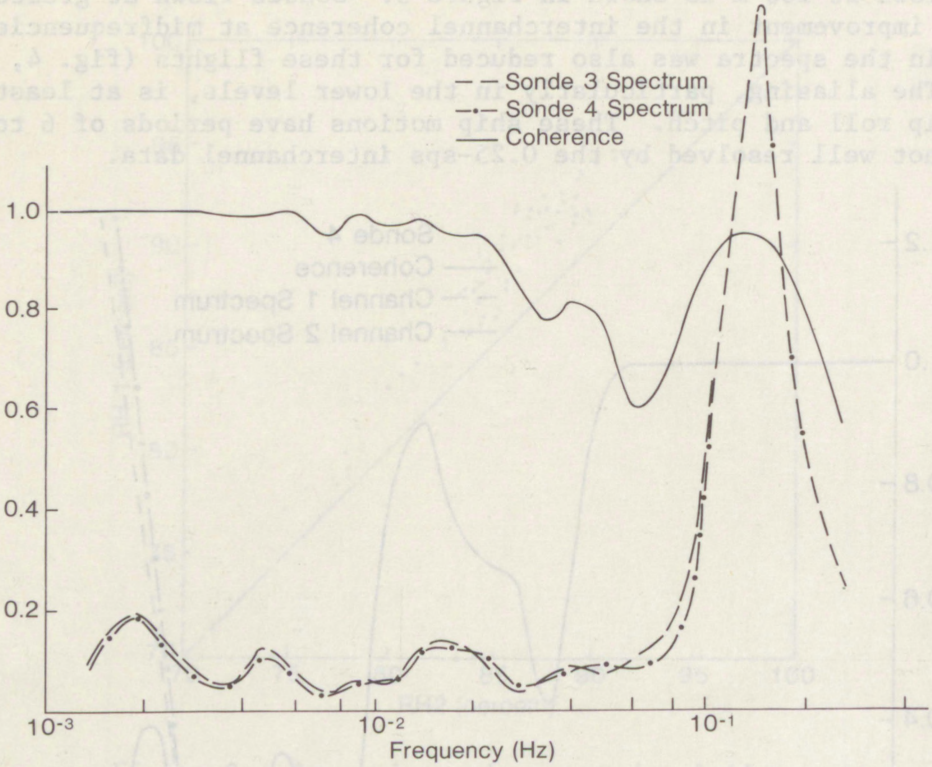

Figure 4.--Wind speed spectra and coherence; 0.25-sps data; interchannel; height, 400 m.

mains high over a broader frequency range than the interchannel coherence but drops off a very high frequency 0.1 Hz). Thus it appears that the 0.5-sps speed data are contaminated by high-frequency noise at this level, but are not susceptible to ship motion. The source of the high-frequency noise cannot be determined with certainty but may be the result of balloon and tetherline motion.

In summary, the analysis of the speed spectra shows that (1) speed spectra from the 0.25-sps, 1-channel data will, in general, be aliased at frequencies above 0.03 Hz; (2) the effects of ship roll and pitch on the 0.5-sps speed spectra are most pronounced for sondes flown near the surface; (3) at heights of 400 m or greater, ship roll and pitch have very little direct effect on the speed spectra but in combination with the balloon motion may induce aliasing. Since ship motion has a period of 6 to 12 s, the speed spectra at heights of less than 400 m will be contaminated for frequencies higher than 0.08 Hz.

B. Wind Direction

The 0.25-sps wind direction spectra (not shown here) were aliased at the higher frequencies and in this regard resemble the 0.25-sps wind speed spectra. The interchannel coherence was low for midfrequencies and high frequencies. This was true for sondes flying at all altitudes.

AWS TECHNICAL LIBRARY
FL 4414
859 BUCHANAN STREET
SCOTT AFB IL 62225-5118

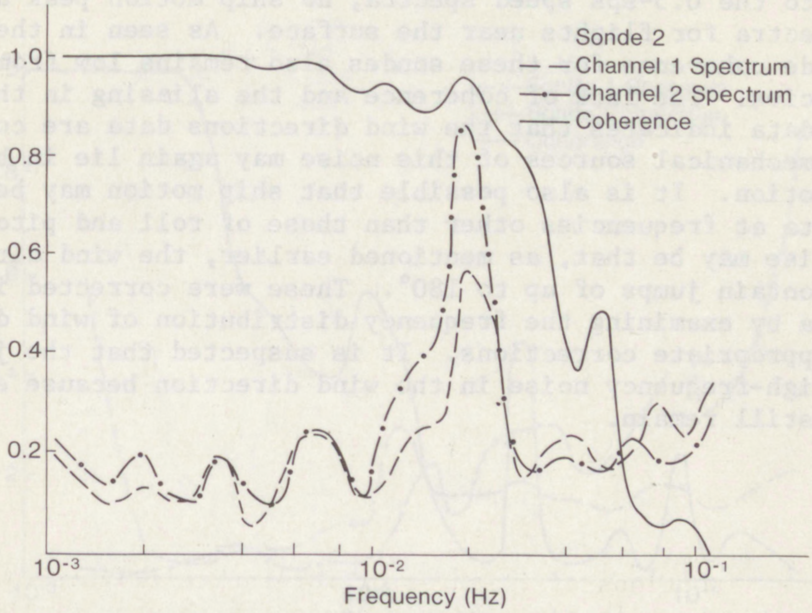

Figure 5.--Wind speed spectra and coherence; 0.5-sps data; intersonde; height, 100 m.

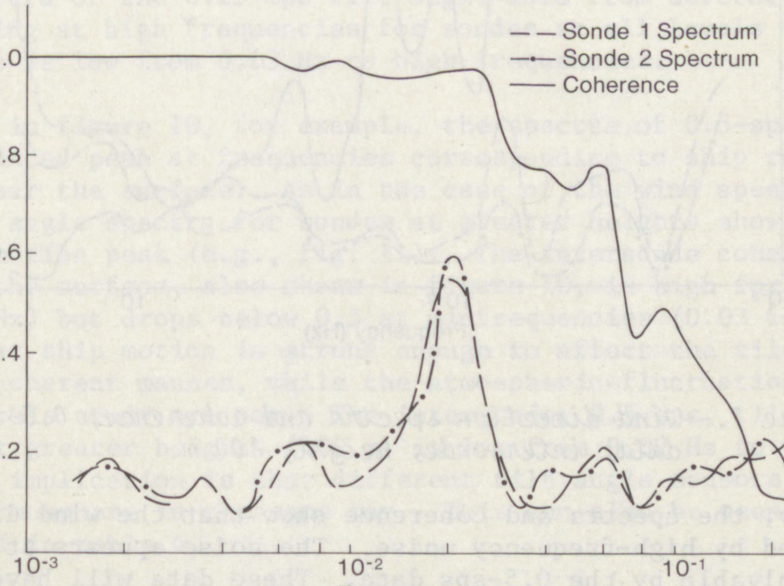

Figure 6.--Wind speed spectra and coherence, 0.5-sps data; intersonde; height, 400 m.

As shown in figures 7 and 8, the 0.5-sps spectra both near the surface and at higher altitudes show aliasing from 0.02 Hz to the Nyquist frequency. In contrast to the 0.5-sps speed spectra, no ship motion peak appears in the direction spectra for flights near the surface. As seen in these figures, the intersonde coherence for these sondes also remains low from 0.02 Hz to high frequencies. The lack of coherence and the aliasing in the spectra for the 0.5-sps data indicates that the wind directions data are contaminated by noise. The mechanical sources of this noise may again lie in balloon and tetherline motion. It is also possible that ship motion may be entering the direction data at frequencies other than those of roll and pitch. Another source of noise may be that, as mentioned earlier, the wind direction data very often contain jumps of up to 180°. These were corrected in processing the BLIS data by examining the frequency distribution of wind direction and making the appropriate corrections. It is suspected that the jumps may contribute to high-frequency noise in the wind direction because errors of a few degrees can still remain.

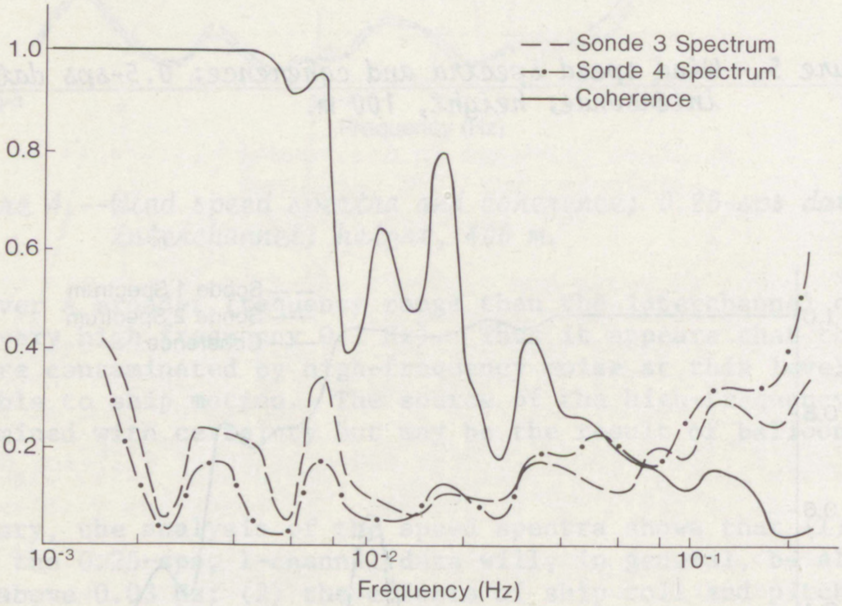

Figure 7.--Wind direction spectra and coherence; 0.5-sps data; intersonde; height, 100 m.

In summary, the spectra and coherence show that the wind direction data are contaminated by high-frequency noise. The noise appears at all heights and is not resolvable by the 0.5-sps data. These data will have to be smoothed, or filtered, for use in some types of analysis. Tests have shown that most of the aliasing can be removed by using a low pass filter with a cutoff frequency of 0.07 Hz.

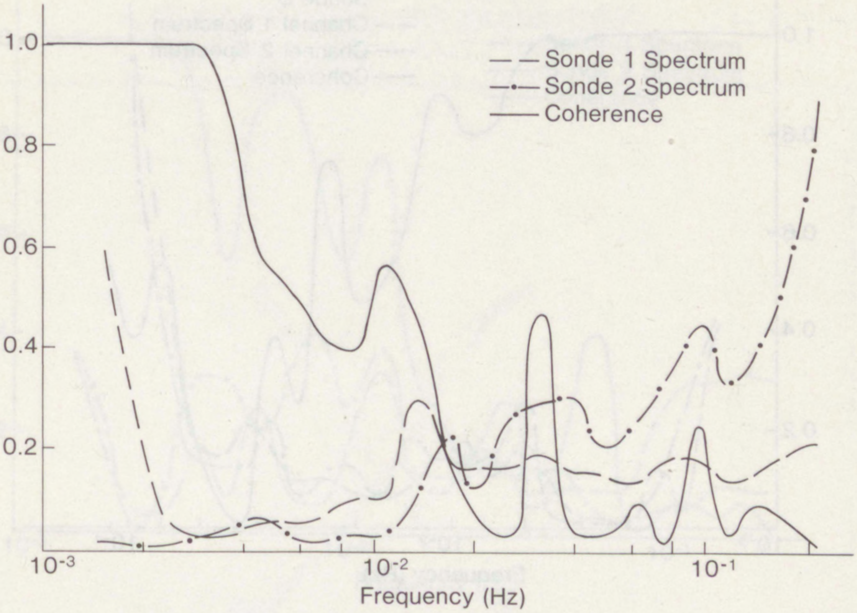

Figure 8.--Wind direction spectra and coherence; 0.5-sps data; intersonde; height, 400 m.

C. Tilt Angle

The spectra of the 0.25-sps tilt angle data from several flights indicate strong aliasing at high frequencies for sondes at all levels (e.g., fig. 9). The coherence is low from 0.03 Hz to high frequencies.

As seen in figure 10, for example, the spectra of 0.5-sps tilt angle data show a pronounced peak at frequencies corresponding to ship roll and pitch for sondes near the surface. As in the case of the wind speed spectra, the 0.5-sps tilt angle spectra for sondes at greater heights show some aliasing but no ship motion peak (e.g., fig. 11). The intersonde coherence of two sondes near the surface, also shown in figure 10, is high for high frequencies (0.1 to 0.2 Hz) but drops below 0.5 at midfrequencies (0.03 to 0.08 Hz). This indicates that ship motion is strong enough to affect the tilt angles of both sondes in a coherent manner, while the atmospheric fluctuations for the flights examined in this study are not. The intersonde, 0.5 sps, tilt angle coherence for sondes at greater heights (400 m) is low from 0.02 Hz to the Nyquist frequency. The implication is that different tilt angle sensors are not responding to the atmosphere in the same way. This can also be seen in the intersonde biases listed in table 4.

5. PROFILES

Five BLIS sondes were flown together in a group with an intersonde spacing of 0.5 m during Researcher flight 51 (Test Run 9) providing an excellent opportunity to compare sonde data during a profile operation in which a rapid

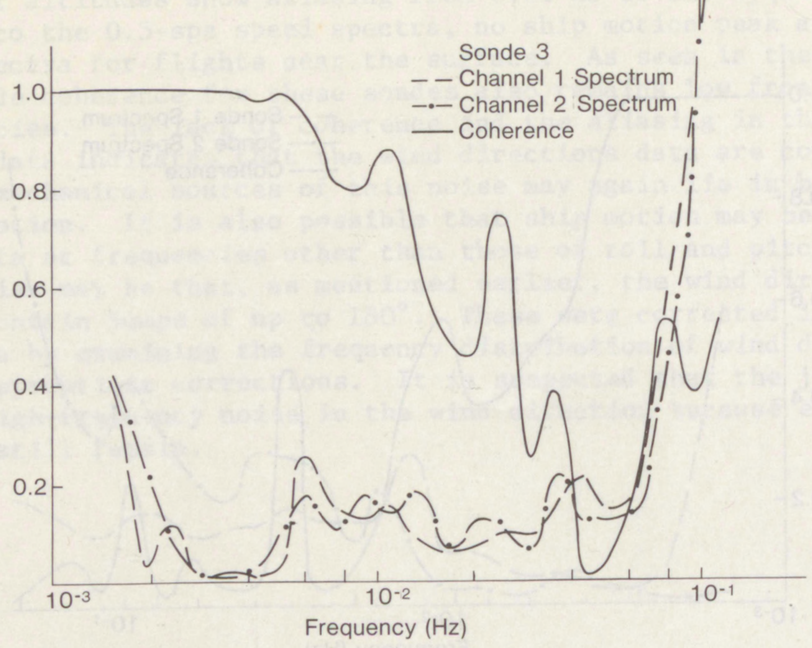

Figure 9.--Tilt angle spectra and coherence; 0.25-sps data; interchannel; height, 100 m.

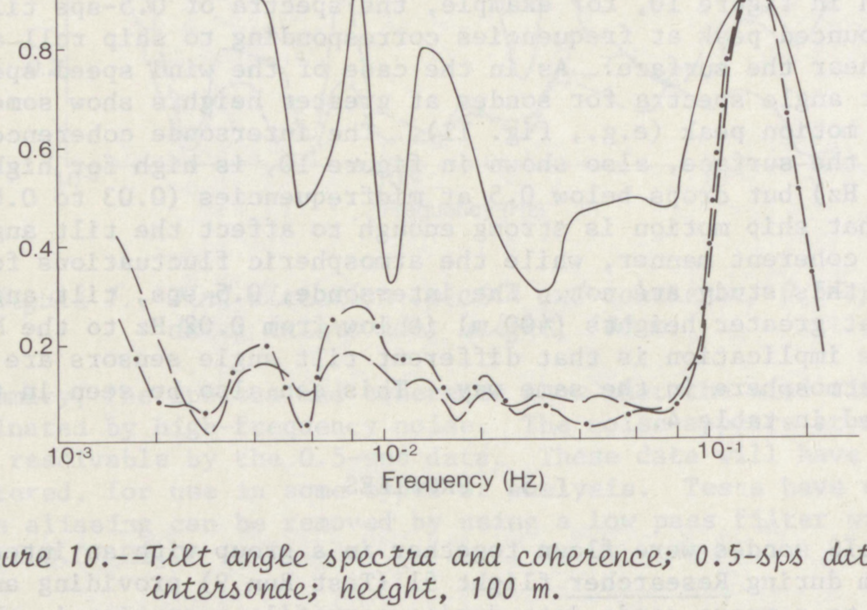

Figure 10.--Tilt angle spectra and coherence; 0.5-sps data; intersonde; height, 100 m.

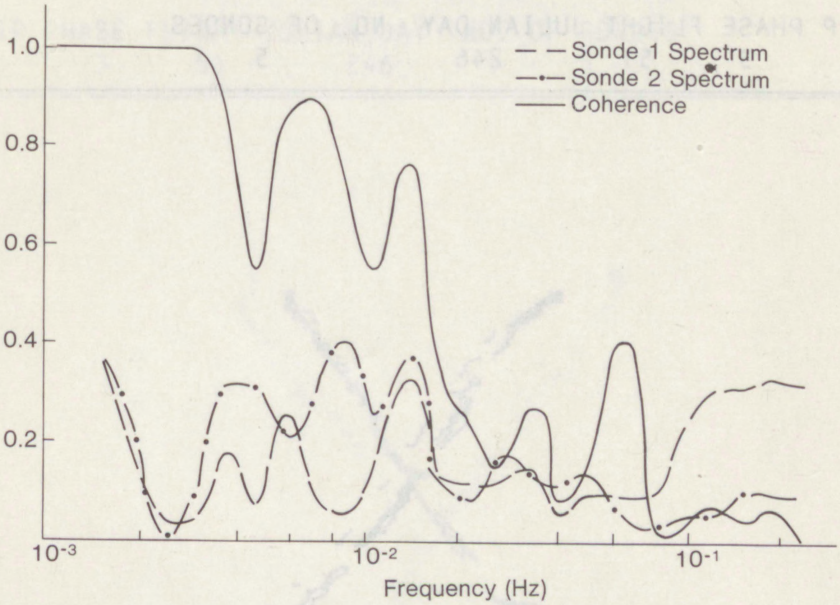

Figure 11.--Tilt angle spectra and coherence; 0.5-sps data; intersonde; height, 400 m.

ascent from the surface to 1100 m was followed by a slower stepwise descent.

A. Dry-bulb Temperature

The dry-bulb temperature profiles from all five sondes for the ascent are plotted in figure 12 and show very similar shapes. The offsets in these profiles at low heights are due to biases in the pressures as measured by each sonde. These sonde biases became smaller as the flight progressed, so that the profiles agree more closely at the top of the sounding than they do at the bottom. During the descent, the profiles remain close together, as seen in figure 12. The descent temperature profiles (fig. 13) show a strong inversion at 650 m, and a superadiabatic layer near 350 m, neither of which appears in the ascent profiles. These features occur at heights corresponding to the level-flight portions of the stepwise descent and are quite probably due to the response of the temperature sensors or to radiative heating. In a laboratory study conducted at the University of Virginia, the thermistors were found to have time constants on the order of 20 s (D. Emmit, personal communication). Thus the superadiabatic layer and inversion shown in the descent profile may be a result of the temperature sensors coming into equilibrium with their new surroundings during the level-flight portions of the descent. Further evidence of a temperature sensor lag can be seen by noting that the temperatures during descent are 0.2 to 0.4°C lower than the corresponding temperatures at given heights in the ascent profile.

The sonde temperatures may also rise in the level portions of the flight because of radiative heating. It is difficult to demonstrate this from the

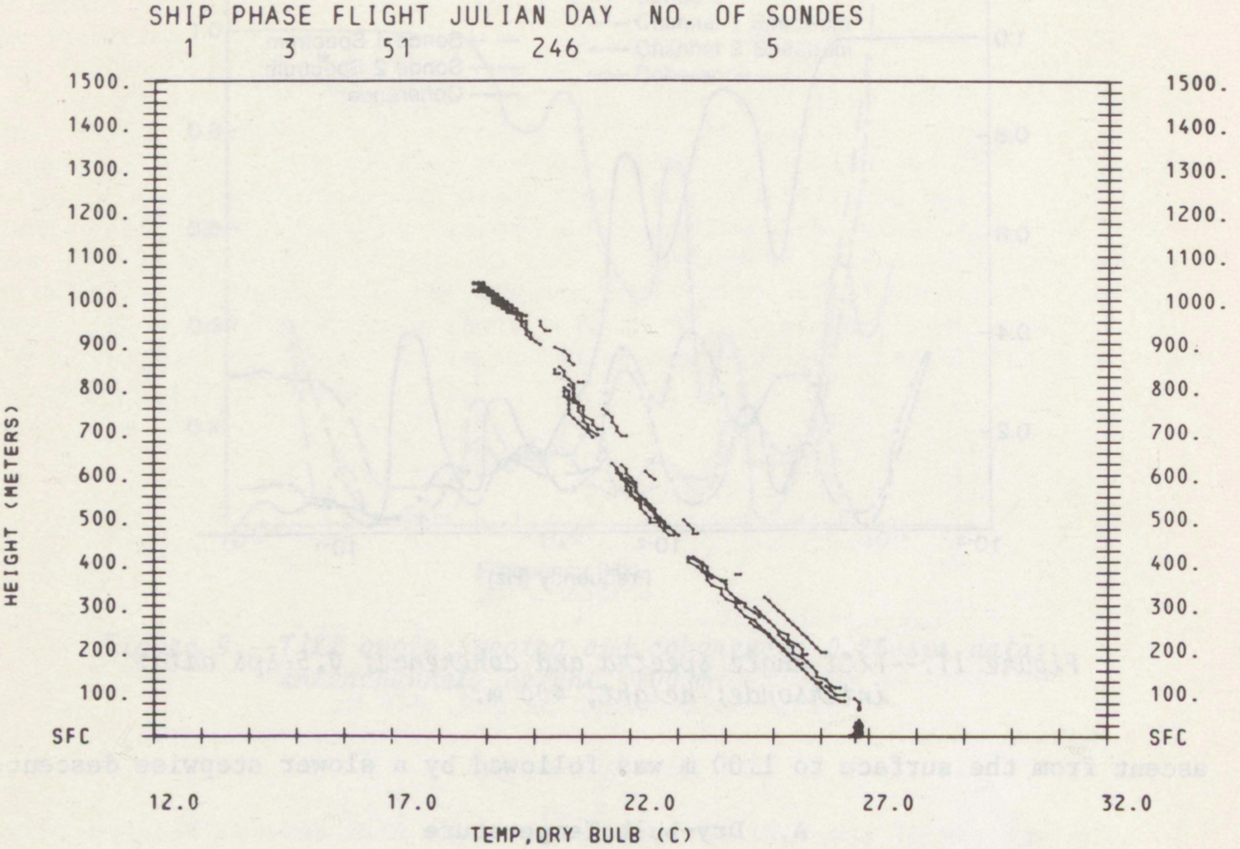

Figure 12.--Dry-bulb temperature profiles; Researcher flight 51; ascent.

data since radiative heating depends on the relative orientation of the sonde and the sun in addition to the cloud cover.

B. Wet-bulb Temperature

The ascent profiles of wet-bulb temperature, presented in figure 14, are similar to those of dry-bulb temperature in their offsets due to pressure biases. The descent profiles of wet-bulb temperature show that the sondes are in close agreement, but the thermistor lag is not as dramatic as for the dry-bulb temperature (fig. 15). The wet-bulb temperatures, however, are slightly lower on descent than at corresponding heights during ascent, indicating the thermistor lag is also present in the wet-bulb sensors.

C. Wind Speed

The wind speed profiles for both ascent (fig. 16) and descent (fig. 17) show that the sondes are in close agreement with each other. The ascent and descent profiles themselves are, however, quite different because the wind sensors measure a component of the sonde motion in addition to the true wind

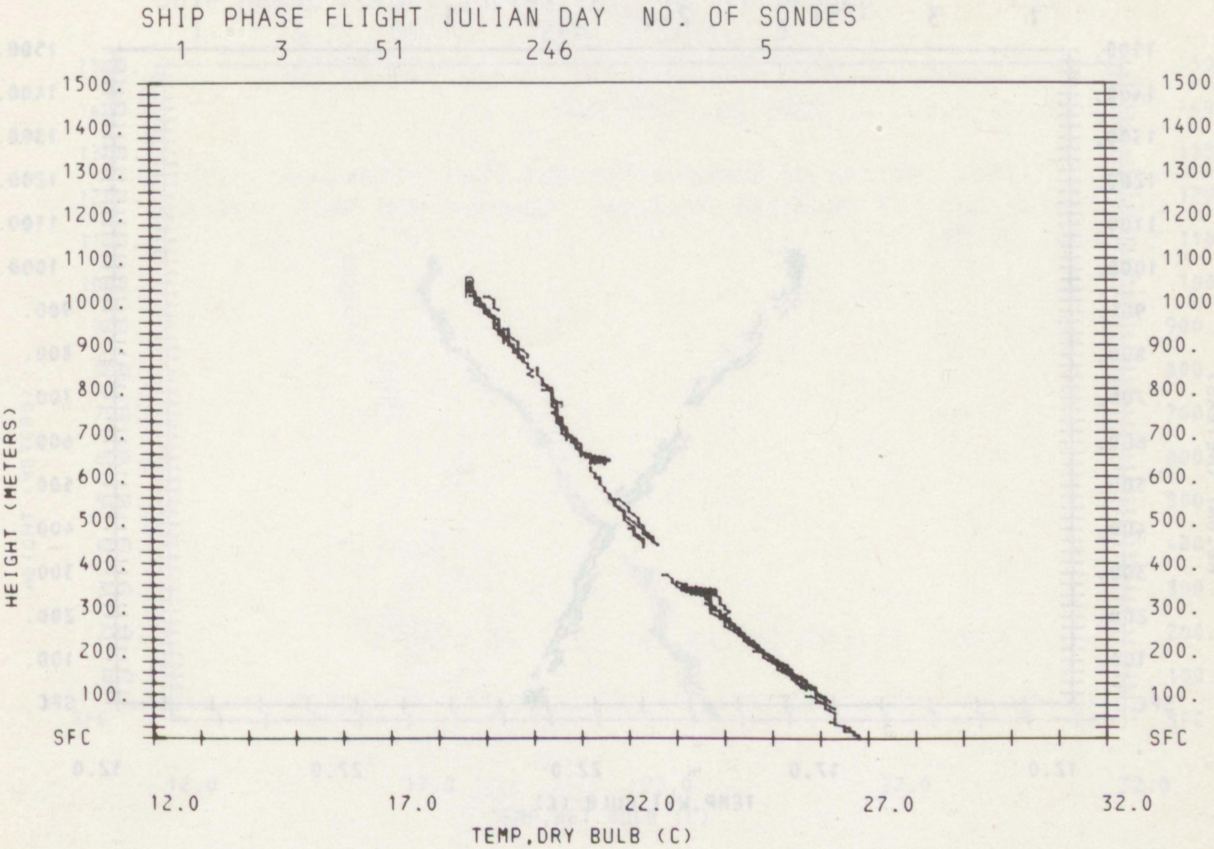

Figure 13.--Dry-bulb temperature profiles; *Researcher* flight 51; descent.

speed. This apparent wind speed is enhanced because the sondes tend to tilt in the direction of motion. Thus for both the ascent and descent profiles the sondes measure a component of the true wind speed and a component due to the ascent or descent rate of the balloon. The shape of the descent wind speed profiles is a result of the stepwise descent procedure, with the wind speed dropping by approximately 2 m/s during the level portion of the flight. The only values of the wind speed not contaminated by balloon motion are those obtained in level flight.

6. DISCUSSION

Analysis of the data from 20 BLIS sondes, roughly one-third of the total number flown during GATE, shows the following:

1) Intersonde relative biases may be quite large, but can be eliminated. Pressure biases however, may be difficult to analyze since the pressure sensors tend to drift.

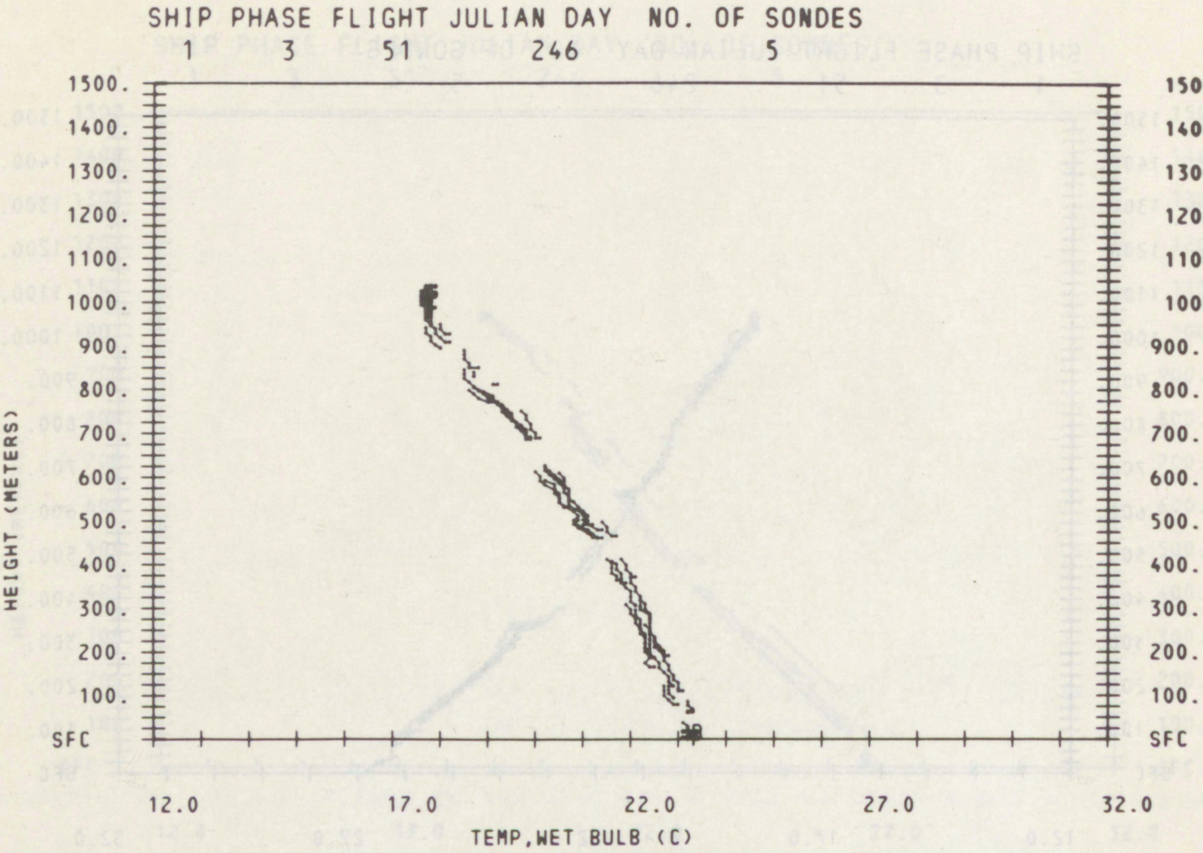

Figure 14.--Wet-bulb temperature profiles; Researcher flight 51; ascent.

2) Root-mean-square errors are relatively small for all sensors.

3) Ship roll and pitch cause aliasing at frequencies above 0.08 Hz in the 0.25-sps wind spectra and a high-frequency peak in the 0.5-sps wind data in cases where the sondes were relatively close to the ship. These effects seem to decrease with height. The wind direction spectra, however, tend to be aliased at frequencies above 0.02 Hz at all levels for both sampling rates.

4) When the BLIS is flown in profile mode, the wind speed and tilt angle are contaminated by the ascent and descent rates of the balloon, and the thermistors show thermal lag and may be affected by radiative heating.

The BLIS data will undoubtedly provide a wealth of new information about the tropical marine boundary layer and illustrate the potential usefulness of tethered sondes for other experiments. The greatest difficulty in using these data will be in the calculation of vertical fluxes by the eddy correlation method. Not only do the tilt angle sensors have rather large relative biases but they are also affected by ship and balloon motion. Very careful filtering techniques will have to be applied in order to obtain meaningful vertical fluxes from the data.

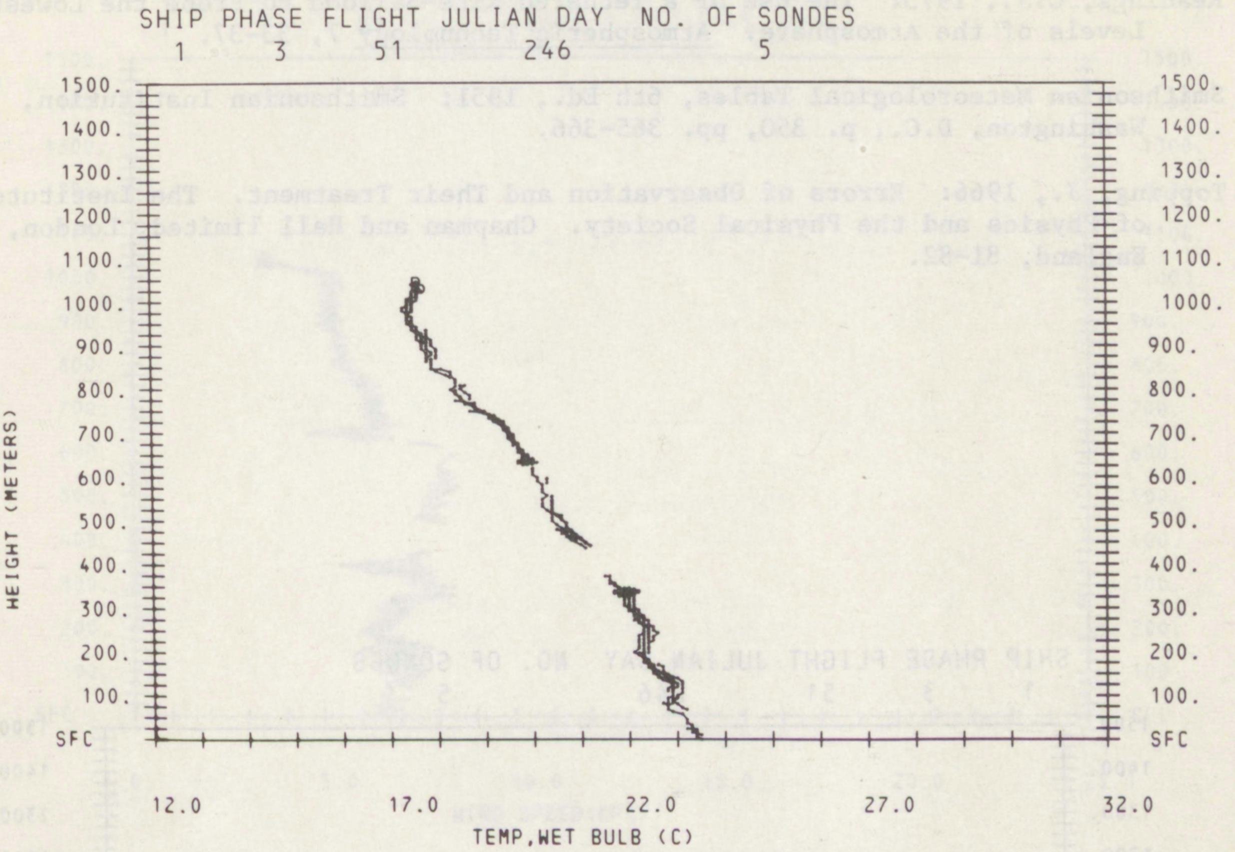

Figure 15.--Wet-bulb temperature profiles; Researcher flight 51; descent.

ACKNOWLEDGMENT

The author wishes to thank the members of the GATE Boundary Layer Advisory Panel for their suggestions in this study.

REFERENCES

Berman, A.E., 1976: Measurements of Temperature and Downwind Spectra in the "Bouyant Subrange". Journal of the Atmospheric Sciences, 33, 495-498.

Burns, S.G., 1974: Boundary-Layer Instrumentation System. Atmospheric Technology 6, 123-128.

Haugen, D.A., J.C. Kaimal, C.J. Readings, R. Rayment, 1975: A comparison of Balloon-Borne and Tower-Mounted Instrumentation for Probing the Atmospheric Boundary Layer. Journal of Applied Meteorology, 14, 540-545.

Readings, C.J., 1975: The Use of a Tethered Kite-Balloon to Probe the Lowest Levels of the Atmosphere. Atmospheric Technology 7, 33-37.

Smithsonian Meteorological Tables, 6th Ed., 1951: Smithsonian Institution, Washington, D.C., p. 350, pp. 365-366.

Topping, J., 1966: Errors of Observation and Their Treatment. The Institute of Physics and the Physical Society. Chapman and Hall limited, London, England, 81-82.

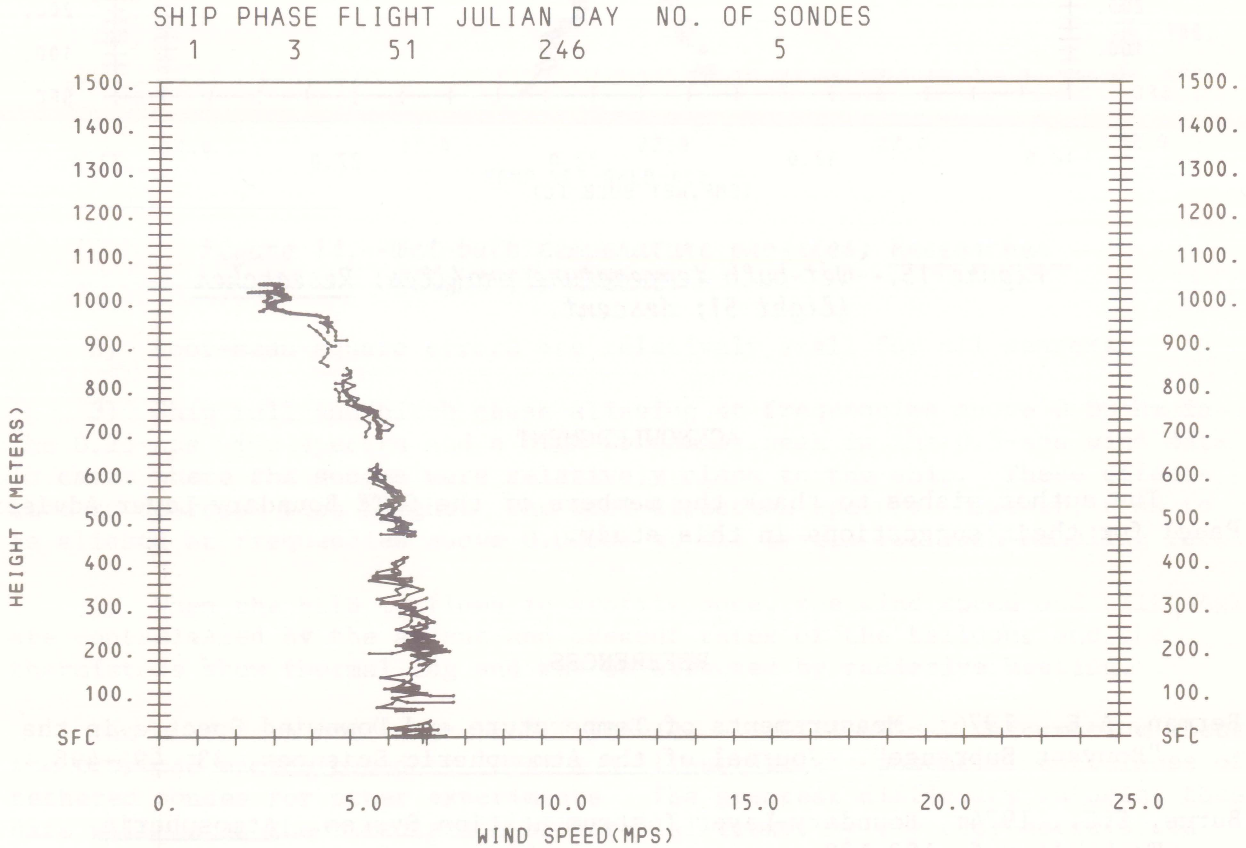

Figure 16.--Wind speed profiles; Researcher flight 51; ascent

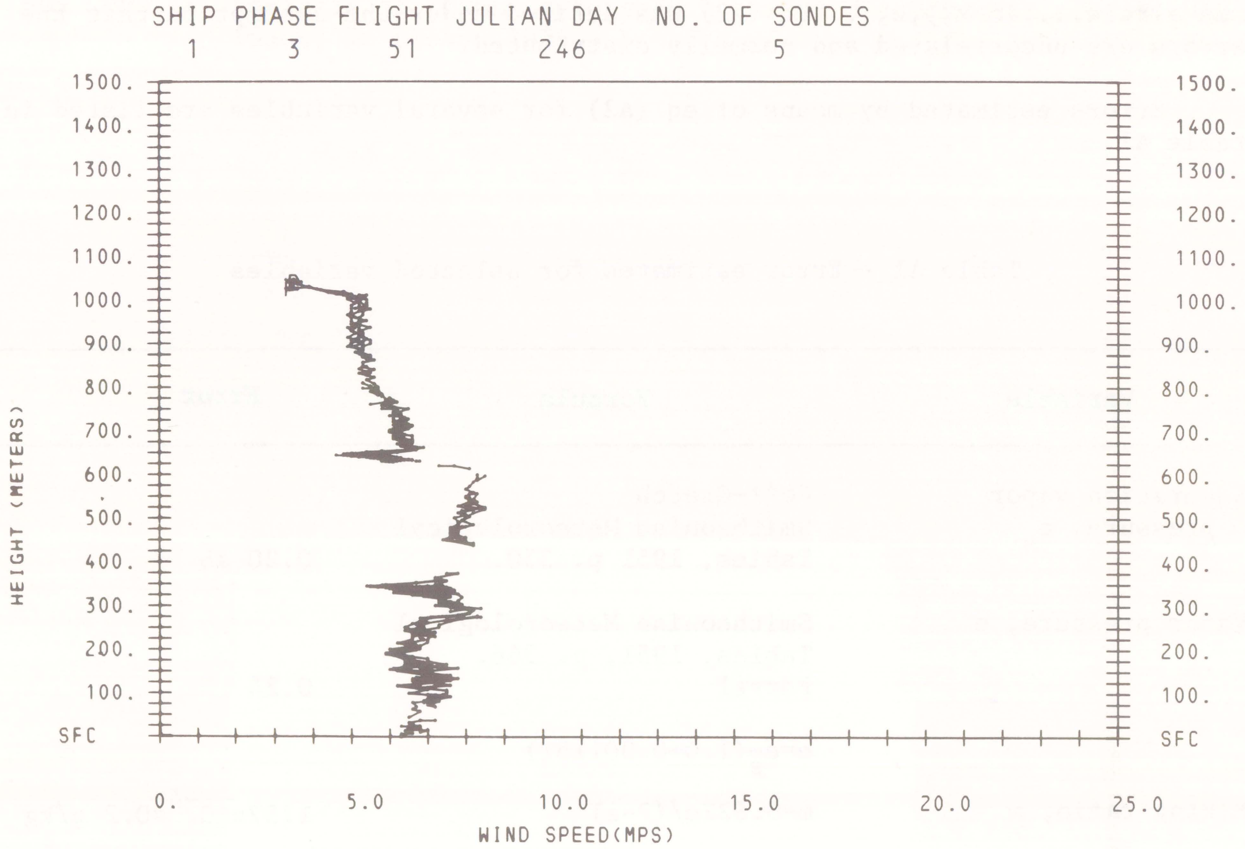

Figure 17.--Wind speed profiles; Researcher flight 51; descent.

APPENDIX

Error Estimates in Derived Variables

The random errors associated with each of the measured variables give rise to errors in the quantities derived from these variables. The rms errors in the measured quantities are discussed in section 2 and are listed in table 3. The errors in the derived quantities can be estimated as follows. Let

$$a = f\,(x,y,z,\ldots\ldots), \qquad (A1)$$

where x,y,z, ...are the variables as measured by the BLIS. The standard error can be obtained from the expression (Topping 1965)

$$E_a^2 = \left(\frac{\partial f}{\partial x} E_x\right)^2 + \left(\frac{\partial f}{\partial y} E_y\right)^2 + \left(\frac{\partial f}{\partial z} E_z\right)^2 + \ldots., \qquad (A2)$$

where E_a is the rms error in the desired variable, a; and E_x, E_y, E_z are the rms errors....in x,y,z,....eq (A2) was derived under the assumption that the errors are uncorrelated and normally distributed.

Errors estimated by means of eq (A2) for several variables are listed in table A1.

Table A1.--Error estimates for selected variables

Variable	Formula	Error
Saturation vapor pressure, e_s	Goff-Gratch Smithsonian Meteorological Tables, 1951 p. 350.	0.20 mb
Vapor pressure, e	Smithsonian Meteorological Tables, 1951, p. 366. Ferrel	0.24
	$e=e_s-(1.0+0.00115T)$	
Mixing ratio, m	$m=0.622e/(P-e)$	$1.57\text{x}10^{-4}\approx0.2$ g/kg
Specific humidity, q	$q=0.622e(P-0.378e)$	$1.71\text{x}10^{-4}\approx0.2$ g/kg
Virtual temperature, T_v	$T_v=T(1.0+0.6m)$	0.11°C
Potential temperature, Θ	$\Theta=T(Poo/P)^k$	0.1 K
Virtual potential temperature, Θ_v	$\Theta_v=T_v(Poo/P)^k$	0.11 K
Equivalent potential temperature, Θ_E	$\Theta_E=\Theta\exp\left(\frac{L\ m}{CpT}\right)$	0.60 K
Height change (ΔZ)	$\Delta Z=-\frac{R}{g}T_v\ln(P_2/P_1)$	2.6 m

U.S. DEPARTMENT OF COMMERCE
National Oceanic and Atmospheric Administration
ENVIRONMENTAL DATA SERVICE
Washington, D.C. 20235

Date : September 13, 1976

Reply to Attn. of: D22

To : All Holders of NOAA Technical Memorandum EDS CEDDA 9

From : C. F. Ropelewski CFR

Subject: Errata

The diagrams described by the captions to figures 4 and 5, pages 12 and 13, should be interchanged; that is, figure 4 should appear above the figure 5 caption and figure 5 above the figure 4 caption.

(Continued from inside front cover)

EDS CEDDA-8 Analysis of IFYGL Rawinsonde Baseline Measurements. Scott Williams, in press, 1976.

/LORD F

AWS TECHNICAL LIBRARY
FL 4414
859 BUCHANAN STREET
SCOTT AFB IL 62225-5118